MAPPING AND COMPARING NATURAL LANDING PADS ON MARS.

J. D. Menges[1], and K. M. Cannon[1] [1]Space Resources Program, Colorado School of Mines, Golden, CO, USA. (jdmenges@mines.edu)

Introduction: Landing a spacecraft on the martian surface without a pre-built landing pad presents specific challenges concerning damage to the lander from landing plume interactions with the surface. These interactions can result in high velocity particle ejecta and surface cratering which can cause lander structural pitting or uneven landing/tipping, respectively. To mitigate and minimize these risks, we are developing a series of SHIELD (Surface Hazard Interaction Efficiencies Limiting Damage) equations for Mars [1]. These equations use data constrained from existing orbital datasets to map where "natural landing pads" might be located which reduce hazards associated with terrain and plume surface interaction. Global SHIELD equations constrain global, lower resolution datasets to map regions with high densities of natural landing pads. Local SHIELD equations constrain localized, higher resolution datasets to map contiguous landing plots and compare proposed landing locations.

Background: The goal of the SHIELD equations is to find and map the largest contiguous landing location that reduces the risks associated with natural landing pad operations while meeting the minimum parameters of the landing craft. The SHIELD equation for localized, high-resolution datasets on Mars is:

$$M_{local} = (M_T + M_S + M_{BD} + M_R)/4$$

The subscripts reflect the following: T, thermal analysis from the Thermal Emission Imaging System (THEMIS) at 100 mpp [2-4, 6]; S and R, slope and roughness analysis from High-Resolution Imaging Science Experiment (HiRISE) imagery at 0.25-1.0 mpp [5]; BD, boulder density (rock abundance) analysis from HiRISE imagery at 0.25-1.0 mpp.

We have constructed a draft Python codebase that pulls the feature/variable data from the remote sensing datasets and determines whether the average value within a specified, predetermined grid square meets the minimum parameter thresholds of each variable.

We will use this code to compare a proposed Starship landing location at Phlegra Montes (PM-1) with the Perseverance Rover landing location at Jezero Crater (JC-1).

Method: Using HiRISE DTM and THEMIS derived thermal inertia data for PM-1 and JC-1, raster images of the datasets were cropped to the extent of the HiRISE DTMs for PM-1 and JC-1. We used raster analysis tools to produce hillshade imagery from the DTMs for use as the basemap imagery in our code.

Using raster analysis tools in QGIS [7], we performed slope and roughness analyses on the DTMs. Additionally, we ran a Topographic Position Index (TPI) on the DTMs as a placeholder for Boulder Density. We will eventually use the python library Martian Boulder Automatic Recognition System (MBARS) to identify, locate, and measure boulders in HiRISE imagery to constrain this variable [8]. A TPI analysis of a DTM raster provides a value of the difference between a central pixel and the mean of its surrounding cells. For the sake of initial boulder analysis on a HiRISE DTM (approximately 1.0 mpp), we assume that a TPI pixel value of +1.0 could possibly represents a 1.0 meter diameter boulder.

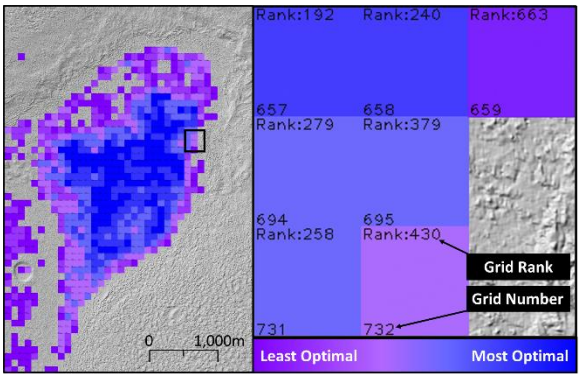

Fig. 1. Ranked slope overlay of PM-1 (left); individual grid square layout (right).

We converted the slope, roughness, TPI, and TI raster imagery to .xyz files (consisting of pixel latitude, longitude, and feature data). Our codebase sets a single grid square size (in this case, 100 x 100 meters) and runs these squares at 100m intervals across the basemap, horizontally and vertically. At each interval, a mean function is run on all the pixels contained within the square for each individual dataset and stored to a list for that square's number. Based on predetermined constraints (e.g., slope must be ≤ 10°), we sort and rank the grid square numbers from most optimal (e.g., slope equals 0º) to least optimal, up to the constraint (slope equals 10°). After individual feature lists are sorted by optimal square number, we can filter the lists to determine which optimal squares are found in all feature lists. When these grid squares are overlayed on the basemap image, we can see the outline of contiguous plots within the

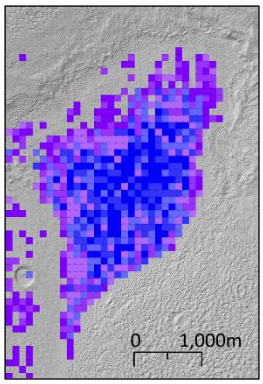

Fig. 2. Ranked average overlay of PM-1, all variables (slope, roughness, TPI, and TI)

proposed landing location that meet the required landing parameters. We created a color overlay for the basemap, which color-codes the grid squares by rank from blue (most optimal) to purple (least optimal while still meeting parameters). Squares that do not meet the parameters are not displayed in the overlay. We can do this for each individual feature. As seen in Fig. 1 for PM-1, each grid square contains a number in the bottom left corner corresponding to the square's location on the basemap. In the top left corner of the square is the rank of that square among all squares meeting the feature parameters. We can also take the average rank for each feature in the final filtered list of squares and sort/rank these grid squares by overall optimal location. Fig. 2 shows the color grid of the optimal locations based on average feature rank for PM-1.

Preliminary Results: In Fig. 3 and Fig. 4, we can compare the contiguous areas at both PM-1 and JC-1 that meet the set parameters for each variable. Nearly all locations at JC-1 meet the SHIELD variable parameters whereas PM-1 is constricted to a smaller area. When we run the grids for each individual variable, we see that the most constricting variable for PM-1 is slope.

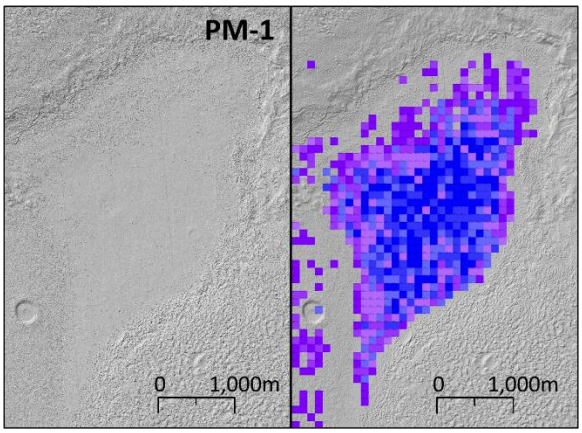

Fig. 4. Hillshade basemap of PM-1 (left); ranked average overlay of PM-1 (right)

The number of grids meeting the parameters in PM-1 is 678 out of a possible 2035 grids, representing 33.3% of the analyzed area. JC-1 contains 1661 of a possible 1705 grids that meet parameters, representing 97.4% of the analyzed area. Based on this analysis, Jezero Crater represents the more optimal landing location.

Discussion: In our current comparison analysis of PM-1 and JC-1, we are determining the more optimal location as a function of the number/percentage of grid squares meeting the parameters. This does not explicitly meet the goal of determining the largest contiguous location. As seen in PM-1, there are standalone grid squares that do not contribute to the largest contiguous area. By manually counting and removing these standalone grids, we get a contiguous area of 604 out of 2035 grids for PM-1 and 1609 out of 1705 grids for JC-1, representing 29.7% (6.04 sq. km) and 94.4% (16.09 sq km), respectively. Further discussion includes adjusting the code to only account for the largest contiguous area instead of manually counting the contiguous grids.

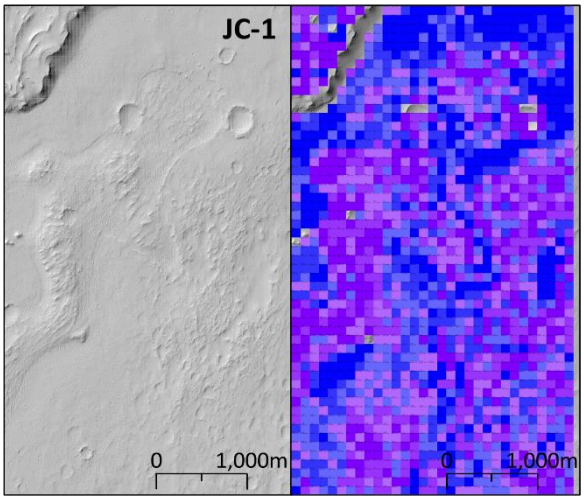

Fig. 3. Hillshade basemap of JC-1 (left); ranked average overlay of JC-1 (right)

Conclusions: The current code works as a proof of concept for qualitative comparisons of natural landing locations on Mars using HiRISE DTMs and THEMIS datasets. Ongoing work will derive quantitative TI values from raw THEMIS datasets [4], adjust the codebase to use linearly stretched SHIELD variables instead of feature data, use CTX/HRSC/MOLA DTM data for locations where HIRISE DTMs are not currently available, and eventually adapt the codebase for natural lunar landing pads.

References: [1] Menges, J.D. (2022) 53rd LPSC, 1559. [2] Fergason, R.L. (2006) JGR, 111(E12). [3] Edwards, C.S. (2008) JGR, 113(E11). [4] Ciazela, M.J. (2021) Remote Sensing, 13(18). [5] UA (2022) HiRISE, uahirise.org. [6] USGS/PDS (2022) Astropedia, astrogeology.usgs.gov. [7] QGIS (2022) QGIS, qgis.org. [8] Hood, D.R. (2019) 50th LPSC, 2132.